Electronic Supplementary Material (ESI) for ChemComm.

Supporting information

Fluorescent zinc and copper complexes for detection of Adrafinil in paper-based microfluidic devices.

Mehmet Gokhan Caglayan,[a,b] Sara Sheykhi,[a] Lorenzo Mosca,[a] Pavel Anzenbacher, Jr.*[a]

[a] Department of Chemistry, Bowling Green State University Bowling Green, OH 43403, USA
[b]Department of Analytical Chemistry, Faculty of Pharmacy, Ankara University, Ankara, Turkey

E-mail: pavel@bgsu.edu

Table of Contents

1. Chemicals and Instrumentation

All chemicals were analytical grade and they were used without purification. All the reactions were carried out under an inert atmosphere (N_2). Fluorescence spectra were measured with an Edinburgh FLS920 single photon counting fluorimeter. Fluorescence images were recorded on a Kodak Image Station 440CF or Kodak Image Station 4000MM PRO instrument. ^{1}H- and ^{13}C-NMR spectra were measured with a Bruker® Avance IITM 500MHz UltraShieldTM (Bruker Corporation, Mass., USA) spectrometer operating at 11.7 T. Mass-spectrometry studies were performed using a Shimadzu MS-8030 equipped with an electron spray ionization (ESI) source and a triple quadrupole mass analyzer or a Shimadzu Axima Performance Matrix assisted laser desorption ionization-time of flight (MALDI-TOF) mass spectrometer. The quantum yields were recorded by using a Hamamatsu Quantaurus QY-C11347 absolute quantum yield integrating sphere.

2. Synthesis

2.1 Synthesis of meso-1,2-diphenyl-N¹,N²-bis(quinolin-2-ylmethylene)ethane-1,2-diamine (1).

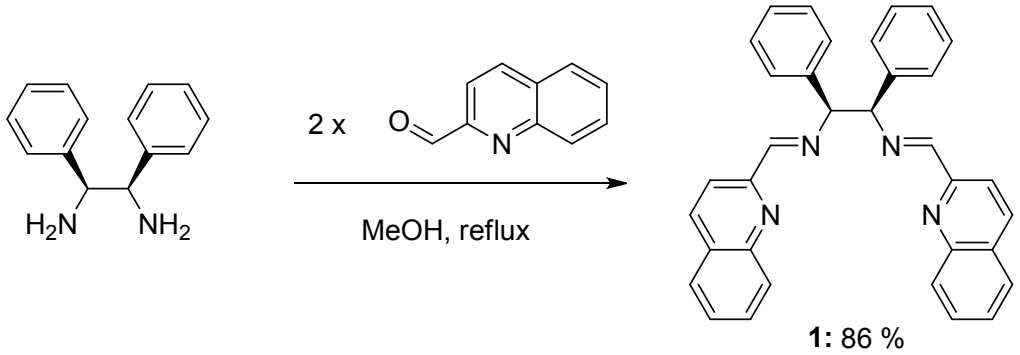

2-Quinolinecarboxaldehyde (222 mg, 1.41 mmol) was suspended in 20 mL of methanol and *meso*-1,2-diphenylethylenediamine (150 mg, 0.706 mmol) was added. The mixture was stirred and refluxed for 12 hours. After this time the reaction mixture was cooled down to room temperature and the yellow precipitate was collected by filtration and washed with diethyl ether. The pale yellow solid was dried in air. The resulting crude material was recrystallized from ethyl acetate to give **1** as a white solid (298 mg, 0.607 mmol, yield: 86%).

^{1}H NMR (500MHz, $CDCl_3$): δ = 8.32 (s, 2H), 8.21 (d, *J*=10Hz, 2H), 8.15 (d, *J*=10Hz, 2H), 8.04 (d, *J*=10Hz, 2H), 7.81 (dd, *J*=7.5Hz, 2H), 7.70 (m, 2H), 7.75 (m, 2H), 7.48 (d, *J*=5Hz, 2H), 7.25 (m, 2H), 7.15 (m, 2H), 5.02 (s, 2H) ppm.

^{13}C NMR (125 MHz, $CDCl_3$): δ = 162.6 (C), 154.8 (CH), 147.7 (C), 140.9 (C), 136.4 (CH), 129.7 (C), 129.5 (CH), 128.8 (CH), 128.3 (CH), 128.2 (CH), 127.7 (CH), 127.4 (CH), 127.3 (CH), 118.6 (CH), 81.2 (CH) ppm.

ESI (*m/z*): $[M+H]^+$: 491.20

2.2 Synthesis of meso-1,2-diphenyl-N^1,N^2-bis(quinolin-2-ylmethyl)ethane-1,2-diamine (2).

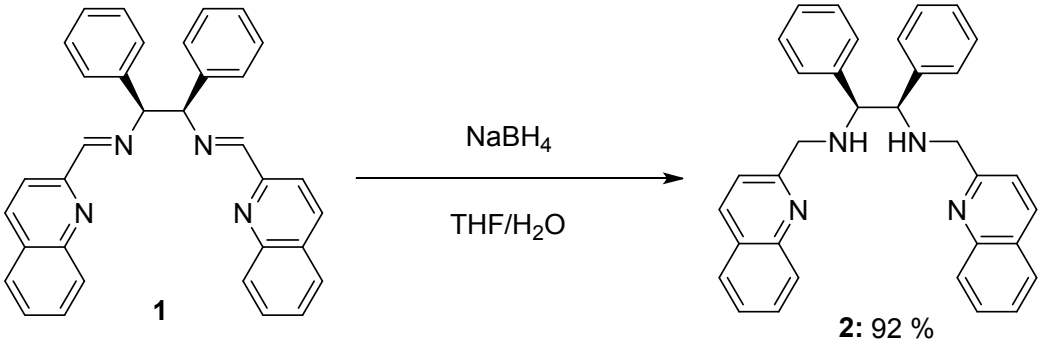

1 (525 mg, 1.07 mmol) was suspended in 100 mL of THF and 25 mL of H_2O. Sodium borohydride (1000 mg, 30 mmol) was added to the reaction mixture gradually (10 × 100 mg). As the reaction progressed, the unreacted **1** dissolved. The reaction mixture was stirred under nitrogen at room temperature for 12 hours. The solvent was removed under reduced pressure and the residue was suspended with 100 mL basic water (saturated $NaHCO_3$) and extracted with dichloromethane (3 × 250 mL). The combined organic extracts were dried over anhydrous Na_2SO_4, filtered, and the solvent removed in vacuo to yield a light yellow-orange solid (487 mg, 0.984 mmol, yield: 92%).

^{1}H NMR (500MHz, $CDCl_3$): δ = 7.99 (d, *J*=7.5Hz, 2H), 7.89 (d, *J*=5Hz, 2H), 7.75 (d, *J*=7.5Hz, 2H), 7.65 (m, 2H), 7.49 (m, 2H), 7.42 (m, 2H), 7.39 (m, 2H), 7.37 (m, 2H), 7.14 (d, *J*=5Hz, 2H), 5.04 (s, 4H), 3.97 (s, 2H) ppm.

^{13}C NMR (125 MHz, $CDCl_3$): δ = 151.54 (C), 147.60 (C), 136.08 (C), 135.75 (CH), 129.26 (CH), 129.01 (CH), 128.85 (CH), 128.50 (CH), 128.28 (CH), 127.47 (CH), 125.93 (C), 125.57 (CH), 120.62 (CH), 68.23 (CH), 53.06 (CH_2) ppm.

ESI (*m/z*): $[M+H]^+$: 495.30

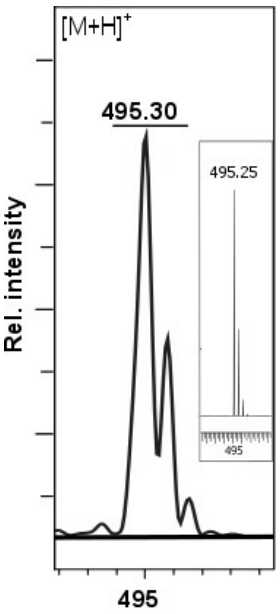

Figure S1. ESI mass spectrum of [***2***+H]$^+$ = 495.30 Inset: Calculated isotope pattern for [***2***+H]$^+$ = 495.25

2.3 Synthesis of (meso-1,2- N,N'-bisquinoline-2-methyl-diphenyl-1,2-diamine) copper(II) trifluoromethanesulfonate (S1).

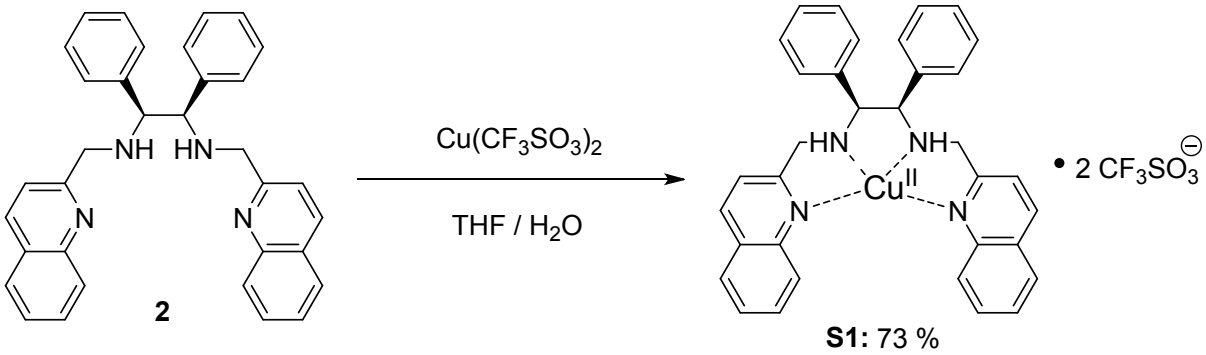

In a 100 mL round-bottom flask, ***2*** (400 mg, 0.808 mmol) was dissolved in 70 mL of THF under nitrogen. Copper(II) trifluoromethanesulfonate (293 mg, 0.808 mmol) was dissolved in 4 mL ultrapure water in a separate round-bottom flask. The two solutions were mixed and stirred under nitrogen for 12 hours. The solvent was removed under vacuum and the resulting dark red solid was dried under high vacuum for 4 hours. The product was washed with diethyl ether, filtered and dried in a desiccator (502 mg, 0.59 mmol, yield: 73 %).

ESI (*m/z*): [*M*+MeOH]$^+$: 592.20

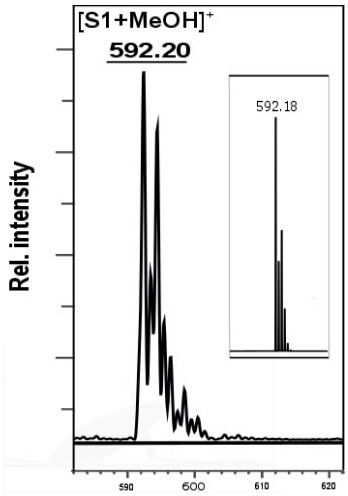

Figure S2. ESI mass spectrum of [*S1*+MeOH]$^+$ Inset: Calculated isotope pattern for [*S1*+MeOH]$^+$ = 592.18

2.4 Synthesis of (meso-1,2- N,N'-bisquinoline-2-methyl-diphenyl-1,2-diamine) zinc(II) trifluoromethanesulfonate (S2).

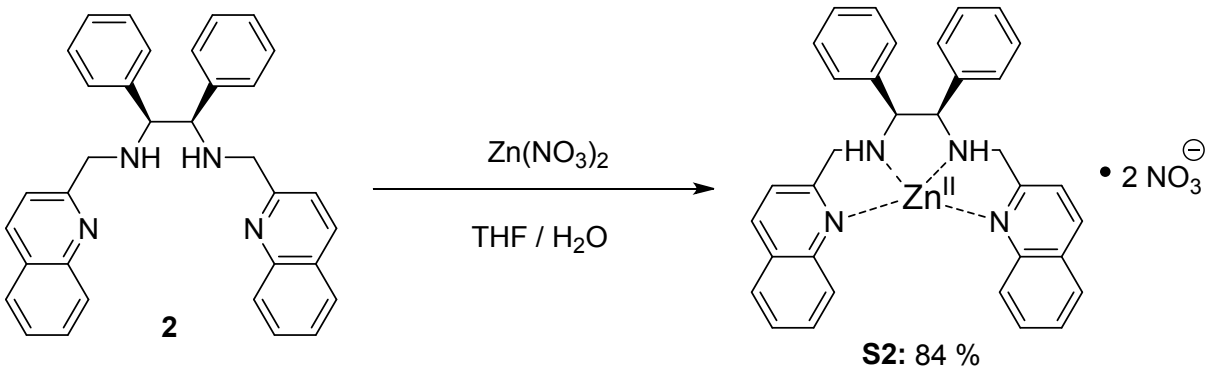

2 (181 mg, 0.368 mmol) was dissolved in 32 mL of THF in a 50 mL round-bottom flask under nitrogen. Zinc nitrate (110 mg, 0.368 mmol) was dissolved in 4 mL ultrapure water in a separate round-bottom flask. The two solutions were mixed and stirred under nitrogen for 12 hours. The solvent was removed under vacuum and the resulting dark yellow solid was dried under high vacuum for 4 hours. Finally, the solid was washed with diethyl ether, filtered and dried in a desiccator (209 mg, 0.31 mmol, yield: 84 %).

^{1}H NMR (500MHz, $CDCl_3$): δ = 8.33 (d, *J*=10Hz, 2H), 8.05 (d, *J*=10Hz, 2H), 7.92 (d, *J*=10Hz, 2H), 7.84 (m, 2H), 7.70 (m, 2H), 7.55 (m, 2H), 7.49 (m, 2H), 7.48 (m, 2H), 7.35 (d, *J*=5Hz, 2H), 5.02 (s, 4H), 2.27 (s, 2H) ppm.

^{13}C NMR (125 MHz, $CDCl_3$): δ = 152.59 (C), 147.94 (C), 137.46 (C), 136.38 (CH), 134.51 (CH), 130.55 (CH), 130.44 (CH), 130.10 (CH), 129.25 (CH), 129.02 (CH), 128.35 (C), 128.18 (CH), 127.91 (CH), 117.40 (CH), 81.19 (CH_2) ppm.

ESI (*m/z*): [*M*+MeOH]$^{+}$: 593.20

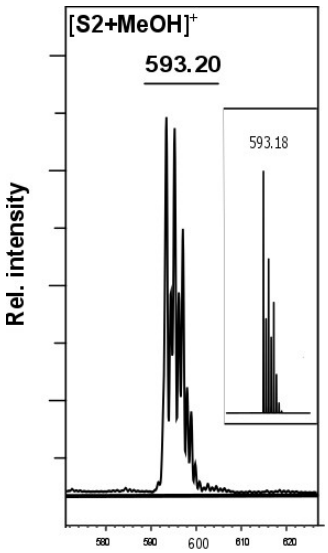

Figure S3. ESI mass spectrum of [*S2*+MeOH]$^{+}$ = 593.20 Inset: Calculated isotope pattern for [*S2*+MeOH]$^{+}$ = 593.18

3. Fluorescence titrations

All solutions were prepared in H_2O/Acetonitrile 3:7 at pH = 6 (MES, 50 mM). The concentrations used were: [S1]= 1.2 mM, [C343] = 1 μM, and [S2] = 20 μM.

3.1 Sensor 1 - titrations

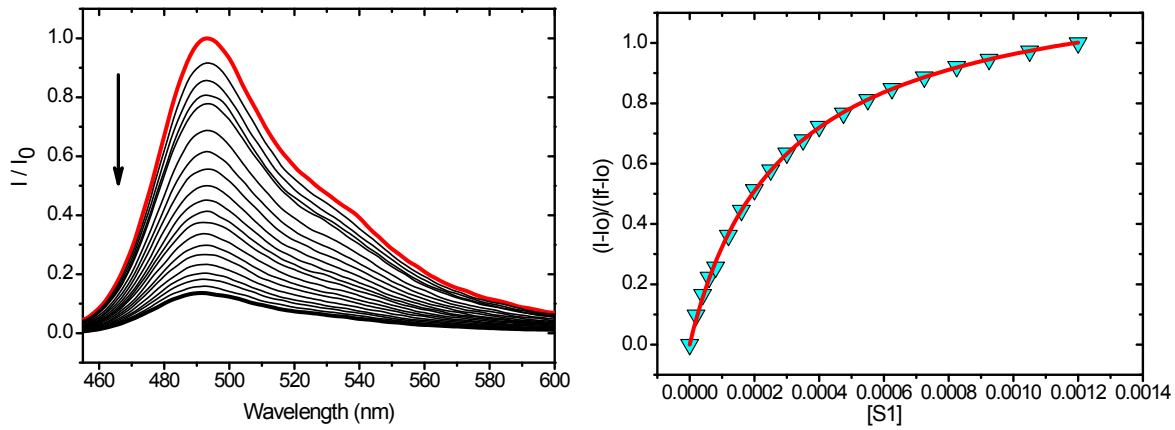

Figure S4. Fluorescence titration spectra and binding isotherm of Coumarin 343 (1 μM) – S1 (λ_{exc} = 444 nm)

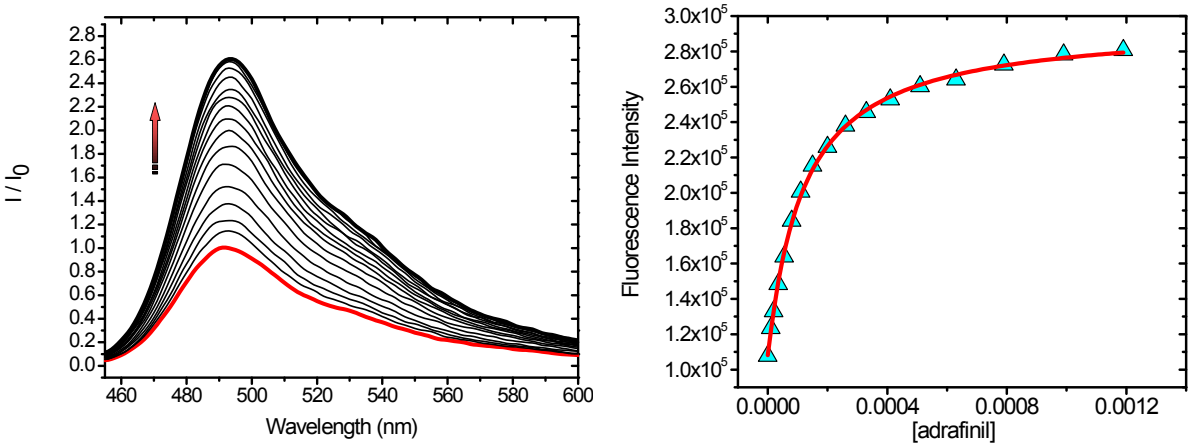

Figure S5. Fluorescence titration spectra and binding isotherm of S1•Coumarin 343 – adrafinil (λ_{exc} = 444 nm)

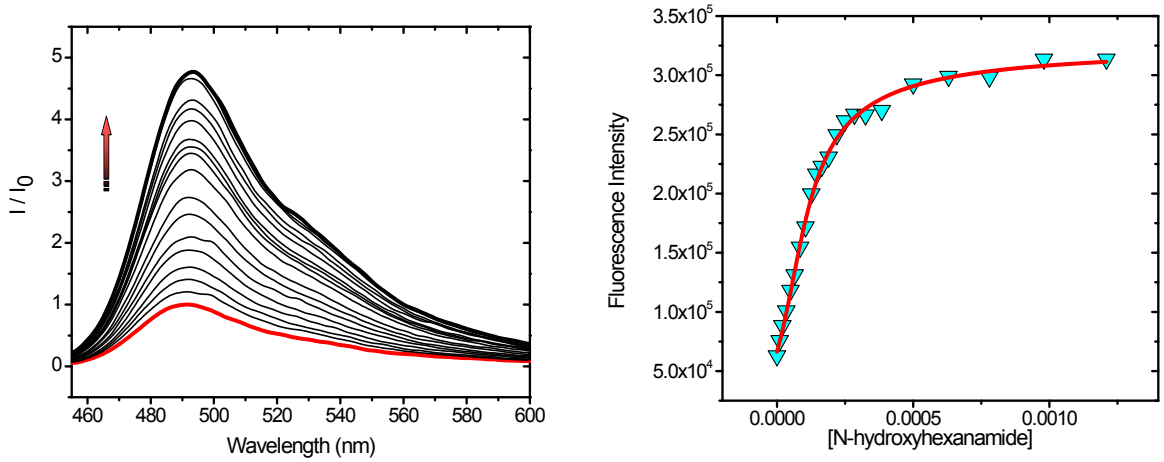

Figure S6. Fluorescence titration spectra and binding isotherm of S1•Coumarin 343 – *N*-hydroxyhexanamide (λ_{exc} = 444 nm)

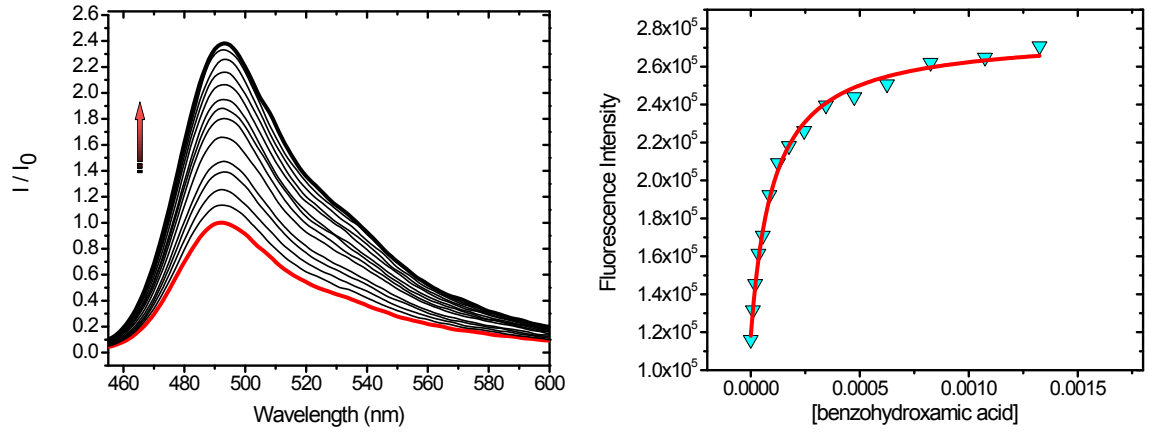

Figure S7. Fluorescence titration spectra and binding isotherm of S1•Coumarin 343 – benzohydroxamic acid (λ_{exc} = 444 nm)

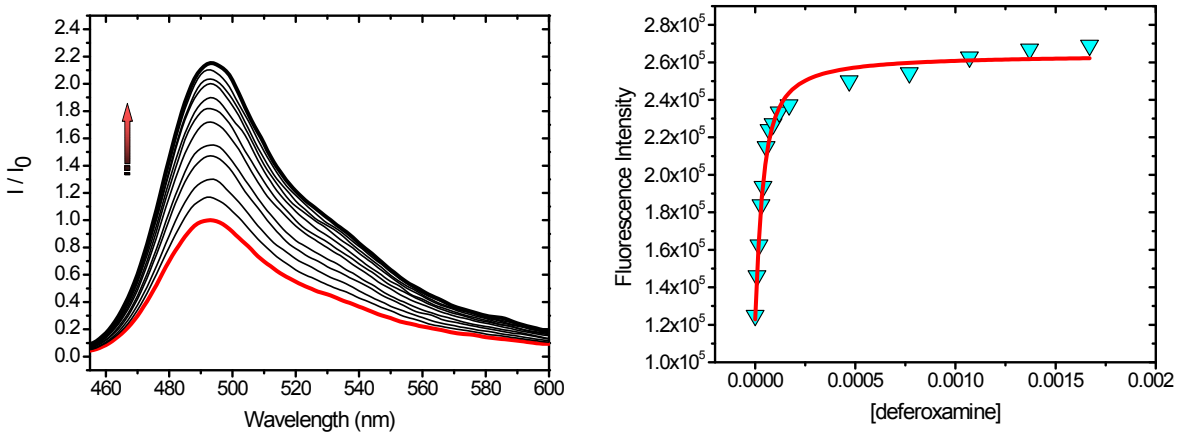

Figure S8. Fluorescence titration spectra and binding isotherm of S1•Coumarin 343 – deferoxamine (λ_{exc} = 444 nm)

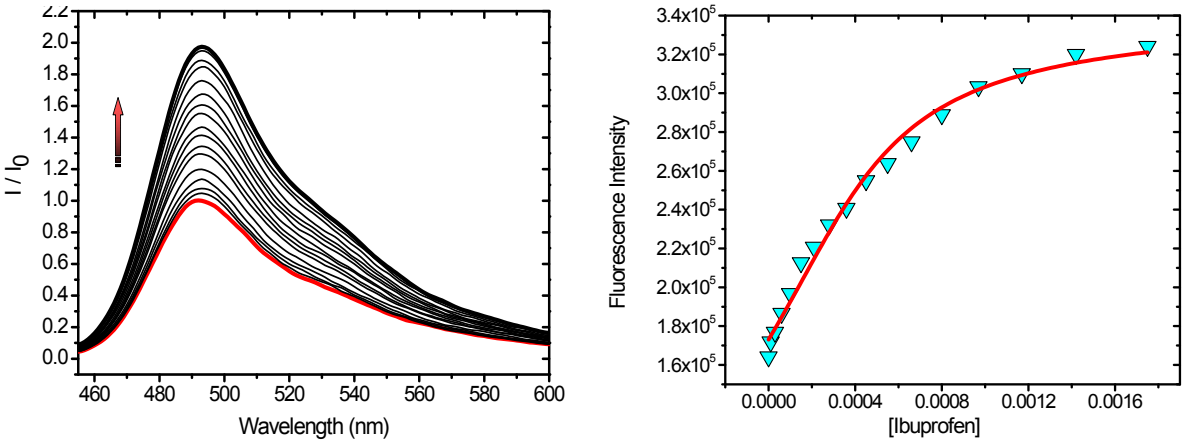

Figure S9. Fluorescence titration spectra and binding isotherm of S1•Coumarin 343 – ibuprofen (λ_{exc} = 444 nm)

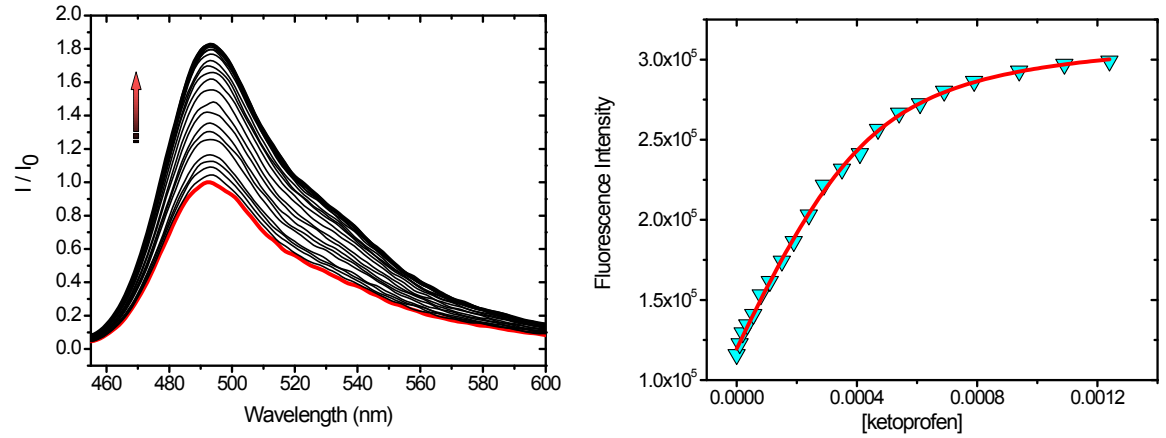

Figure S10. Fluorescence titration spectra and binding isotherm of S1•Coumarin 343 – ketoprofen (λ_{exc} = 444 nm)

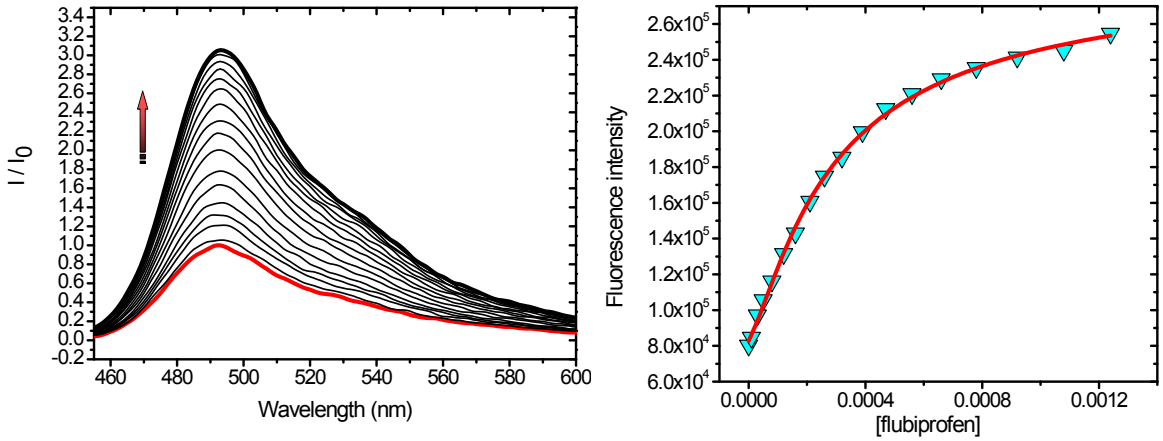

Figure S11. Fluorescence titration spectra and binding isotherm of S1•Coumarin 343 – flurbiprofen (λ_{exc} = 444 nm)

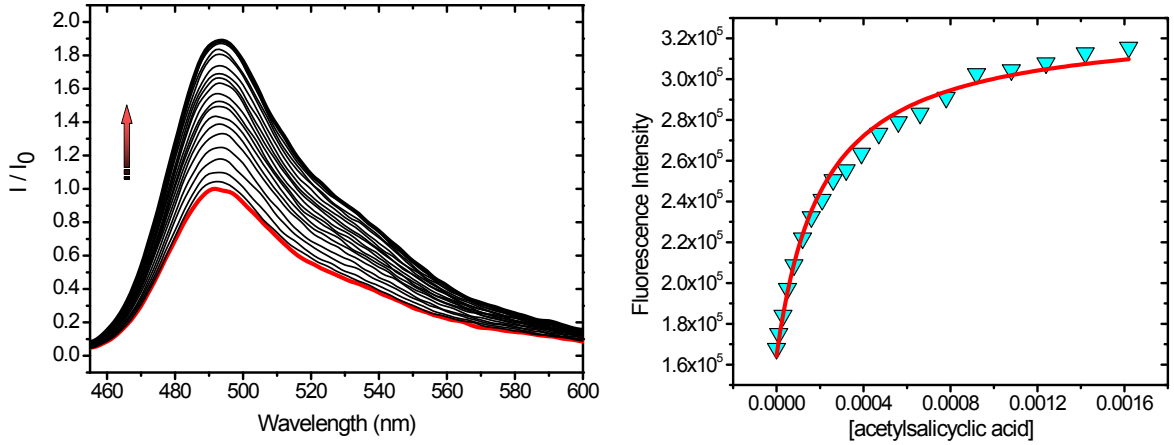

Figure S12. Fluorescence titration spectra and binding isotherm of S1•Coumarin 343 – acetylsalicyclic acid (λ_{exc} = 444 nm)

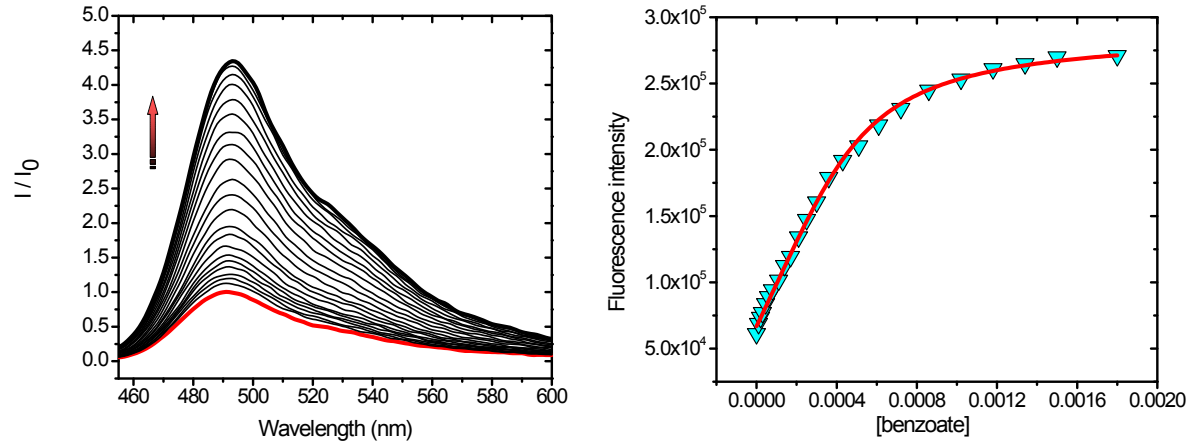

Figure S13. Fluorescence titration spectra and binding isotherm of S1•Coumarin343 – benzoate (λ_{exc} = 444 nm)

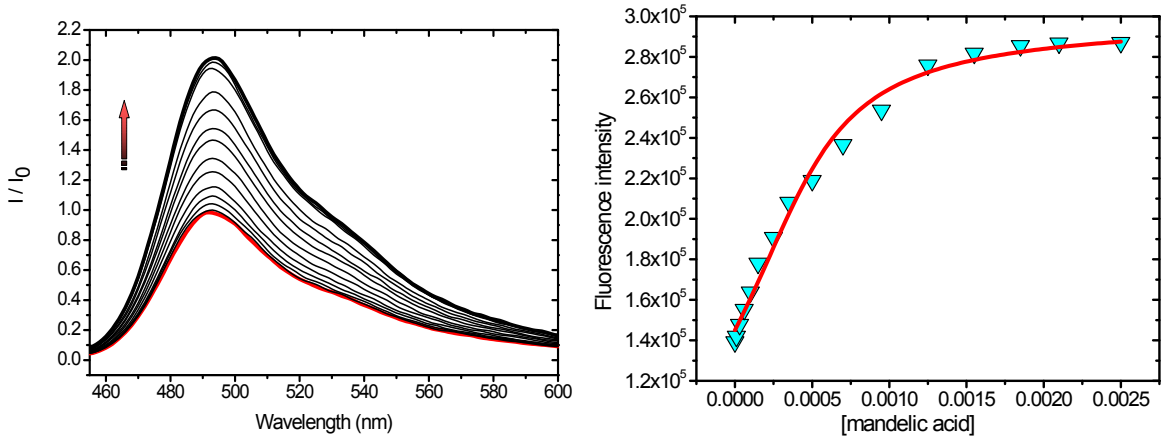

Figure S14. Fluorescence titration spectra and binding isotherm of Coumarin 343•S1 – mandelic acid (λ_{exc} = 444 nm)

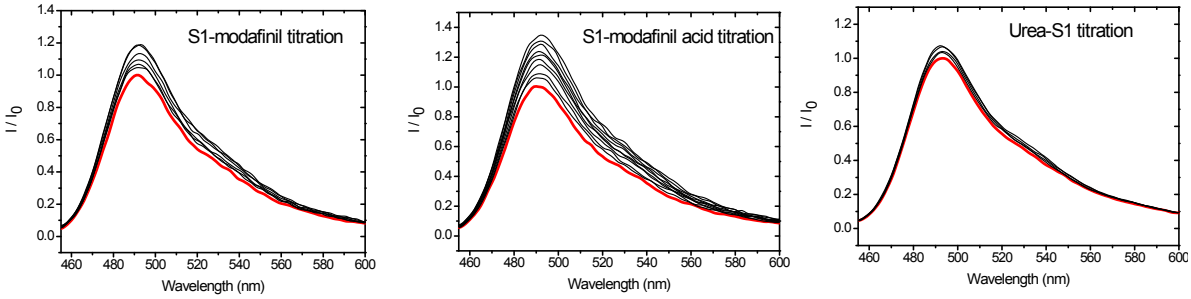

Figure S15. Fluorescence titration spectra of S1•Coumarin343 and a) modafinil b) modafinil acid c) urea (λ_{exc} = 444 nm)

3.2 Sensor 2 - titrations

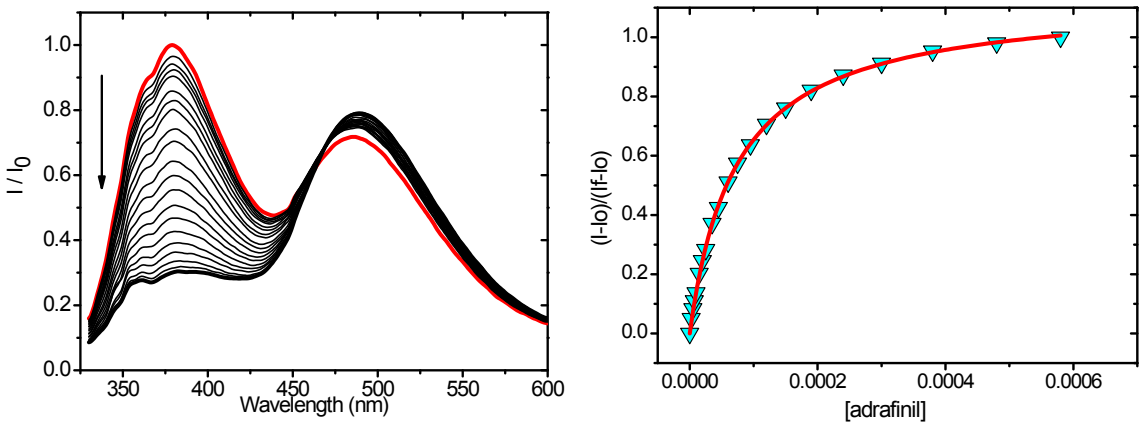

Figure S16. Fluorescence titration spectra of S2 and adrafinil (λ_{exc} = 320 nm)

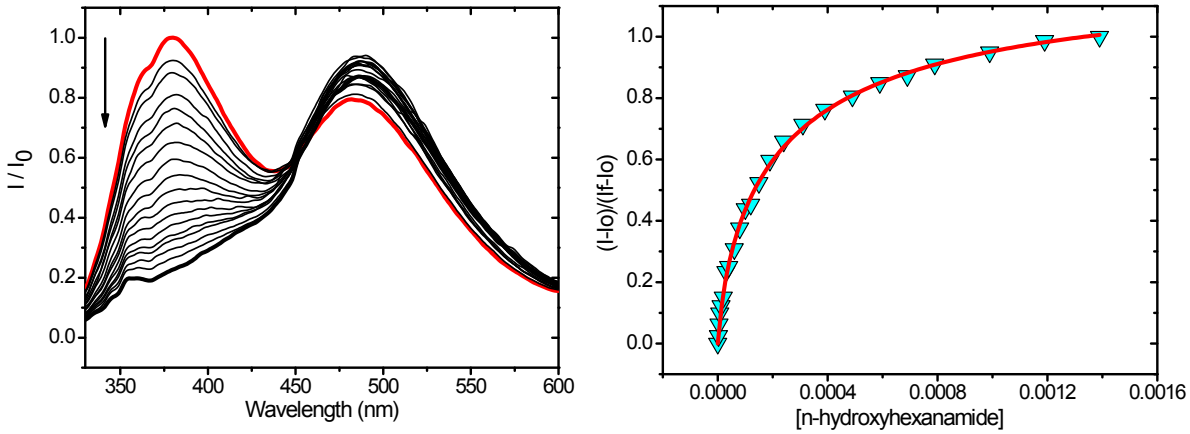

Figure S17. Fluorescence titration spectra of S2 and *N*-hydroxyhexanamide (λ_{exc} = 320 nm)

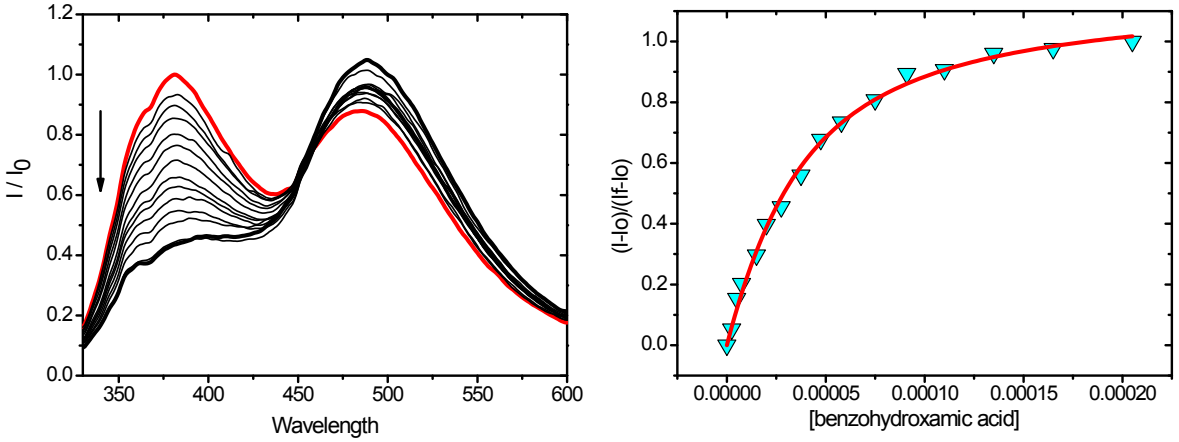

Figure S18. Fluorescence titration spectra of S2 and benzohydroxamic acid (λ_{exc} = 320 nm)

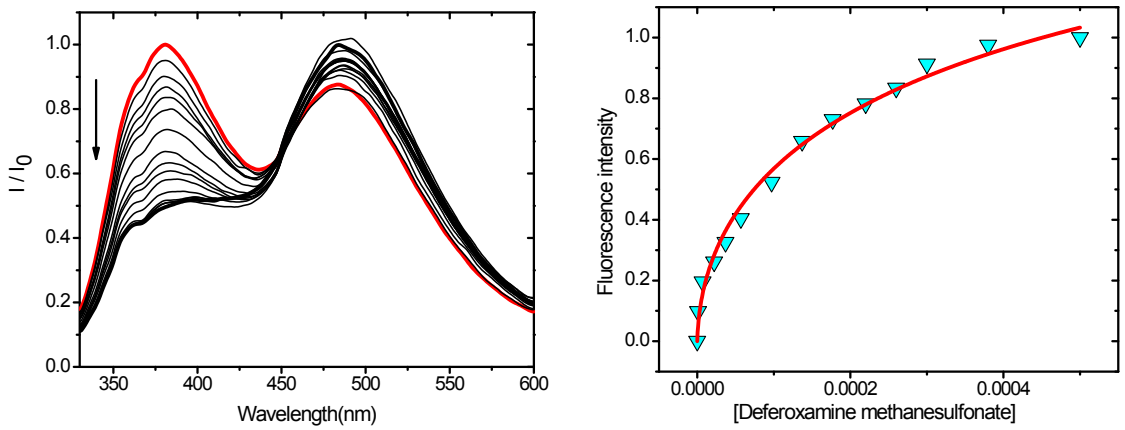

Figure S19. Fluorescence titration spectra of S2 and deferoxamine (λ_{exc} = 320 nm)

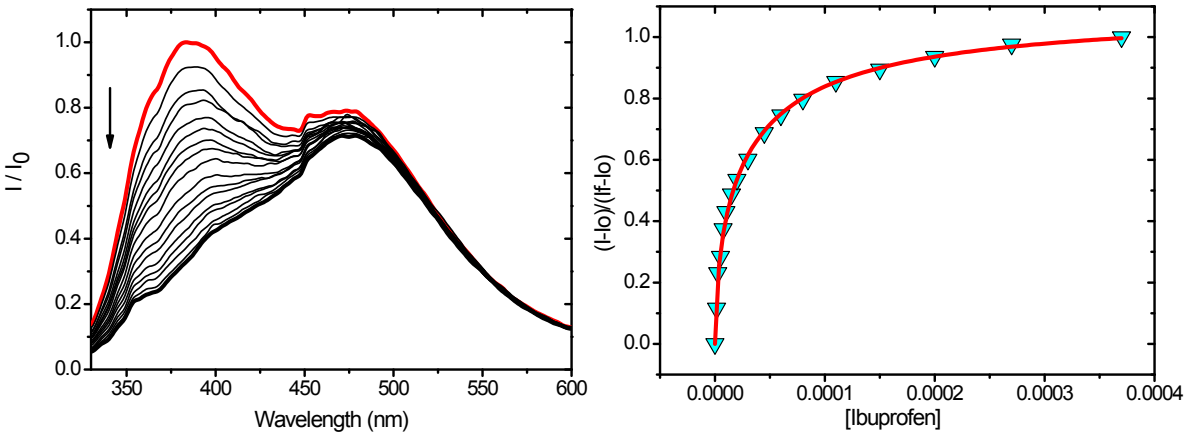

Figure S20. Fluorescence titration spectra of S2 and ibuprofen (λ_{exc} = 320 nm)

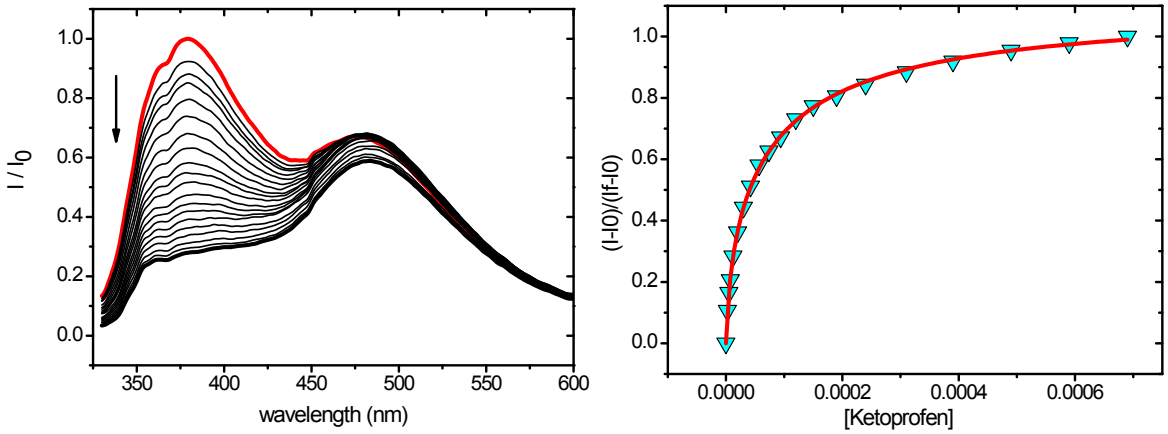

Figure S21. Fluorescence titration spectra of S2 and ketoprofen (λ_{exc} = 320 nm)

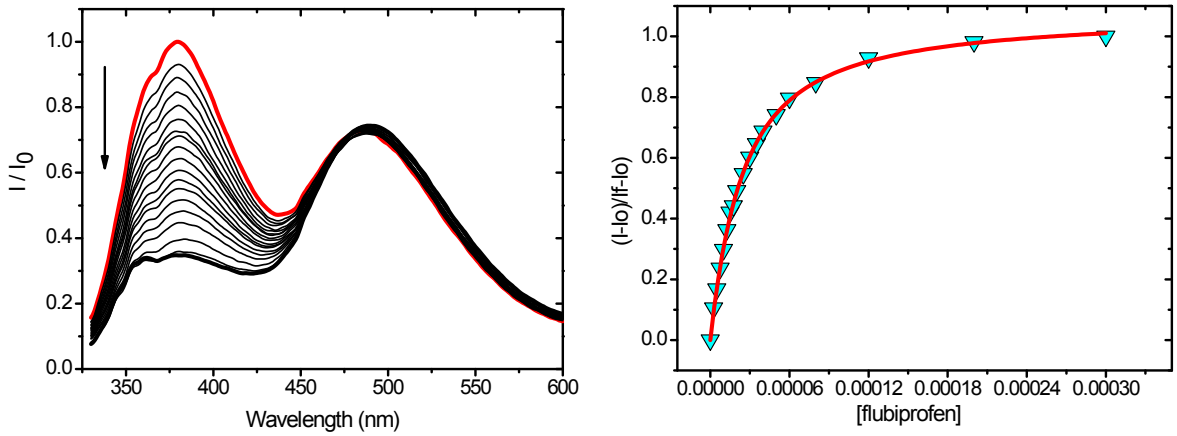

Figure S22. Fluorescence titration spectra of S2 and flurbiprofen (λ_{exc} = 320 nm)

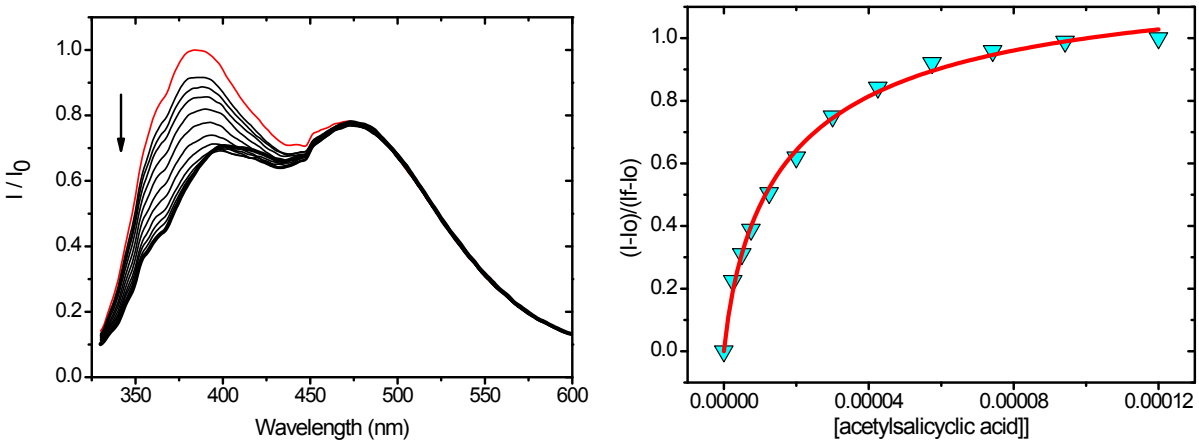

Figure S23. Fluorescence titration spectra of S2 and acetylsalicyclic acid (λ_{exc} = 320 nm)

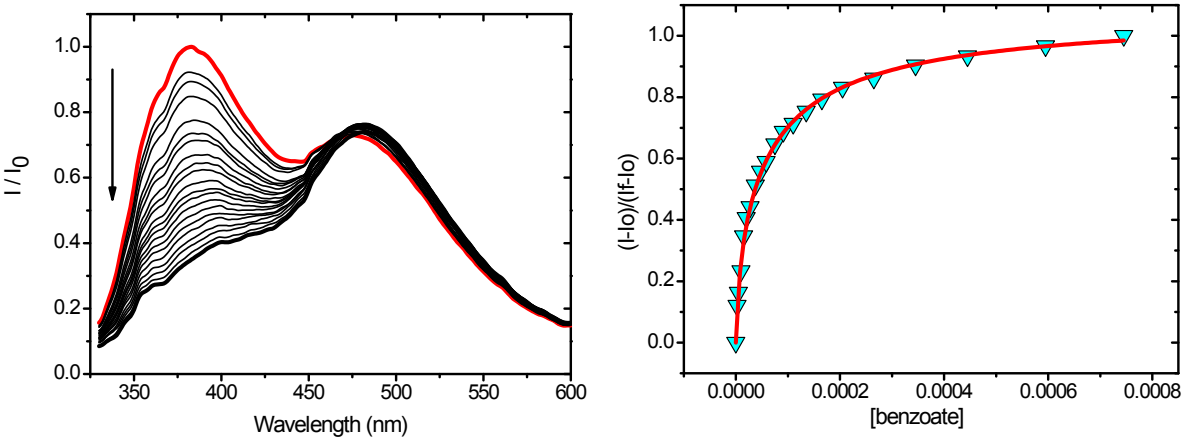

Figure S24. Fluorescence titration spectra of S2 and benzoate (λ_{exc} = 320 nm)

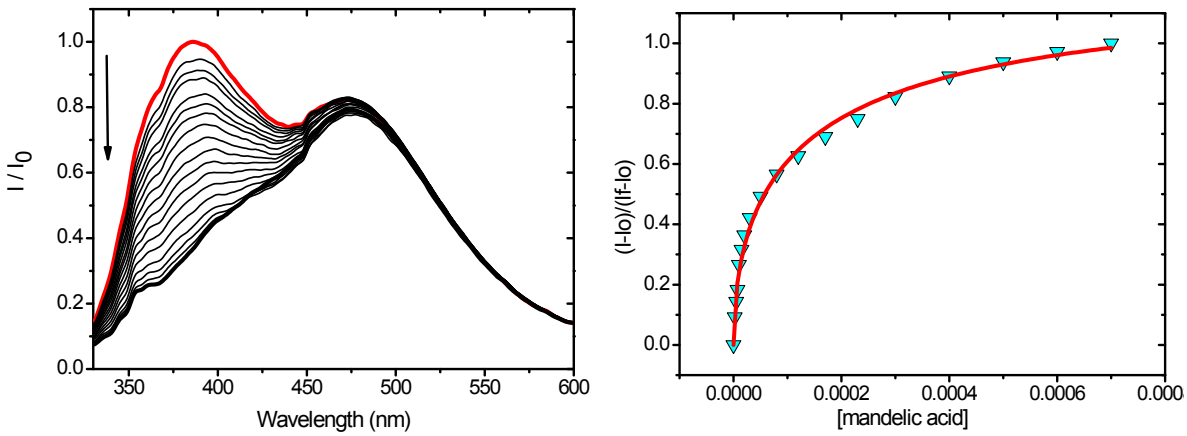

Figure S25. Fluorescence titration spectra of S2 and mandelic acid (λ_{exc} = 320 nm)

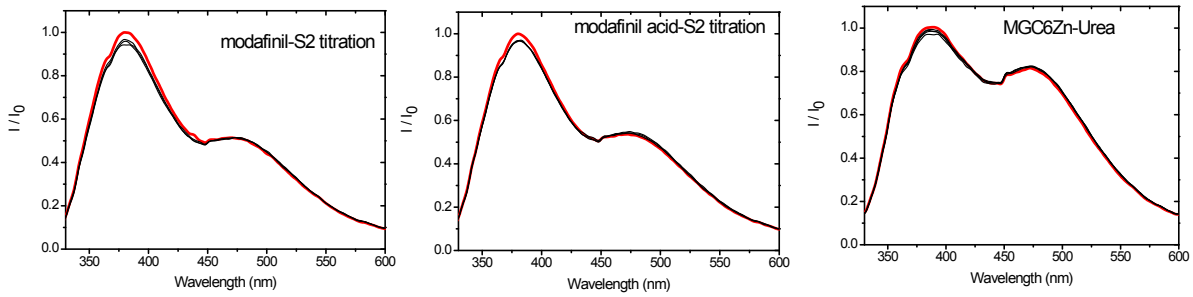

Figure S26. Fluorescence titration spectra of S2 and a) modafinil b) modafinil acid c) urea (λ_{exc} = 320 nm)

4. Sensors-analyte complex study

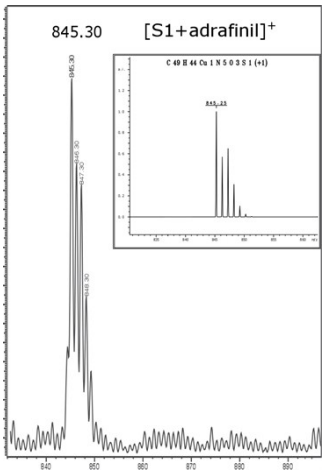

Figure S27. ESI mass spectrum of $[S1+adrafinil-H]^+$ = 845.30, Inset: Calculated isotope pattern for $[S1+adrafinil-H]^+$ = 845.25

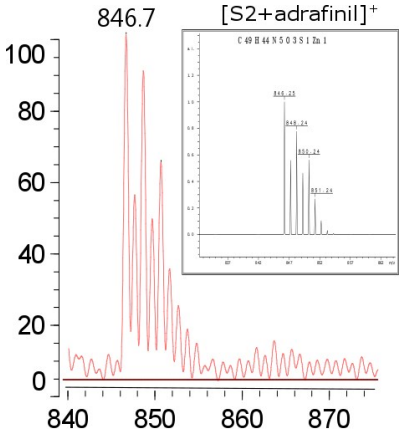

Figure S28. MALDI-TOF mass spectrum of $[S2+adrafinil-H]^+$ = 846.7, Inset: Calculated isotope pattern for $[S2+adrafinil-H]^+$ = 846.3

5. ^{1}H-NMR titration of *N*-hydroxyhexanamide with S2.

Unfortunately, adrafinil is not particularly soluble in the concentrations required to perform NMR titrations, even in DMSO-d6. We perfomed the titrations using a highly soluble analogue, *N*-hydroxyhexanamide (we assume that the oxygen of the sulfoxide group does not participate in coordination to the metal centre). In the figure below, characteristic peaks of the hydroxamate are highlighted. The broad signal at 10.3 ppm is assigned to the −OH group, while at 8.8 ppm we can observe the broad signal of the −NH group. Both signals are broad and in exchange with the solvent. Upon addition of the S2 complex (Zn(II)), both the signals become sharper. This first effect is attributed to the coordination to the Zn(II) that is known to rapidly accelerate the exchange rate of acidic protons upon coordination. A second effect observed is the moderate shift of the two signals. The −OH proton undergoes a moderate downfield shift due to the electrostatic effect of Zn(II) and the increase in acidity of the O−H bond. On the other hand, the −NH proton is expected to undergo an upfield shift due to the increased electron density upon delocalization of the −OH (and C=O) electrons to the nitrogen atom. A −0.15 ppm upfield shift was observed for the −NH proton. The more deshielded methylene group of the aliphatic chain in *N*-hydroxyhexanamide also undergoes a moderate dowfield shift, most likely due to the electrostatic, through-bond and through-space effect of the proximity to the Zn ion. Noteworthy is the loss of coupling in the signal, indicating that the *N*-hydroxyhexanamide is in fast exchange between the complexed (with S2) and uncomplexed form, as expected for Zn(II) complexes ($k_{ex} > 10^{-8}$ s^{-1}). For this reasons we believe that the hydroxamic acids provide the −OH and C=O oxygen atoms as donors and behave as bidentate ligands.

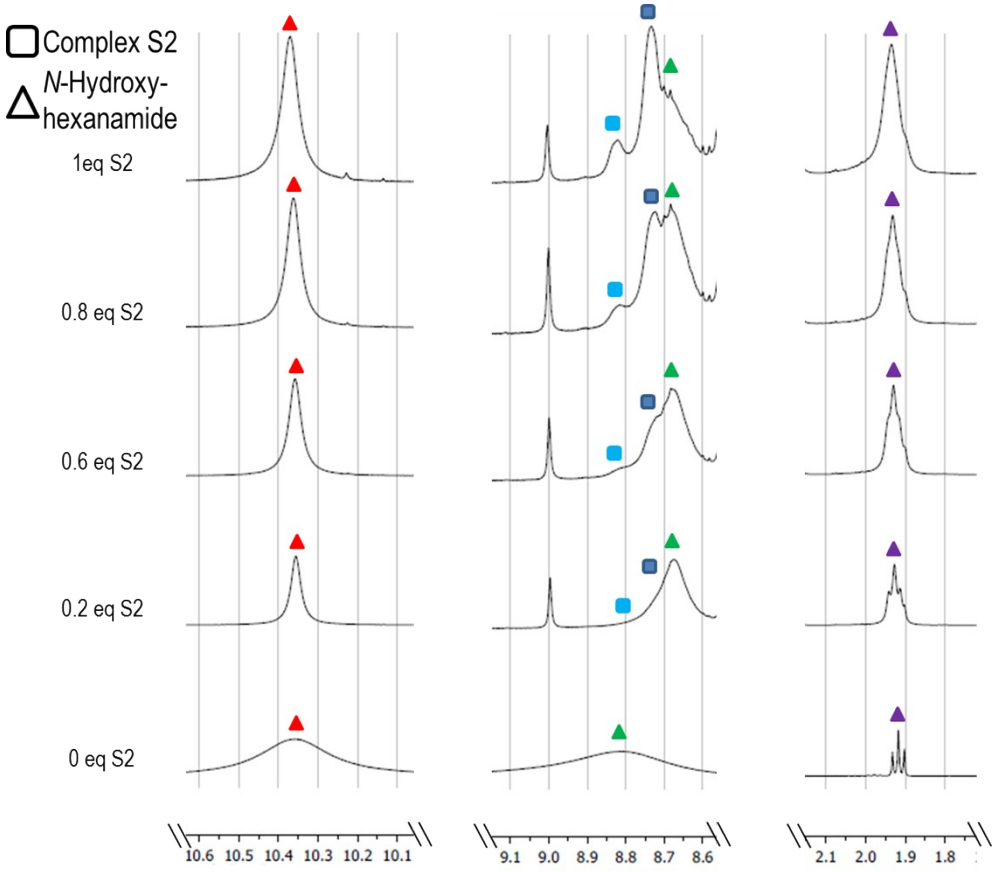

Figure S29. Selected spectral features obtained during the course of the ^{1}H–NMR titration of *N*-hydroxyhexanamide (2.5 mM) with S2 in DMSO-d6.

6. Paper microzone plates study

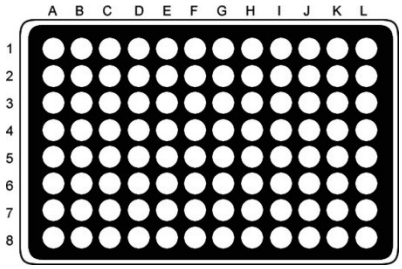

Figure S30. Paper microzone plate used in sensor arrays

The plates were printed on chromatography paper (Whatman) with a Xerox ColorQube model 8570 wax printer. The diameter of a zone on paper microzone plates was 2.95 ± 0.04 mm and the total size of the plate was 53.1 ± 0.36 × 34.3 ± 0.17 mm. After printing, it was baked in an oven for 4.5 minutes at 110 ^{o}C allowing for the penetration of wax into the paper. Finally, the back side of the paper was covered with tape and the paper plates were ready to use for sensor arrays. These plates were utilized for qualitative classification of analytes and quantitative analysis of adrafinil in MES buffer (50 mM, pH 6). For both sensor arrays, the sensors were added on microzones: for S1 detection, 200 nL of coumarin 343 dye (100 μM) was applied on the test zones followed by 2×200 nL of S1 (1 mM) which quenched the fluorescence of the dye. For S2 test zones, 2×200 nL S2 (1 mM) were applied.

In qualitative analysis, 1 mM solutions of each analytes (adrafinil, modafinil, modafinil acid, ibuprofen, ketoprofen, flurbiprofen, acetyl salicyclic acid, *N*-hydroxyhexanamide, benzohydroxamic acid, deferoxamine, benzoic acid and mandelic acid) were prepared in H_2O/Acetonitrile 3:7 at pH = 6 (MES, 50 mM). Then 200 nL of each analyte were added on the zones and the fluorescence images were recorded. Fluorescence intensities were classified by using Linear Discriminant Analysis (LDA). Validation of the analysis was confirmed with cross validation and 100% classification was achieved (Table S1).

In quantitative analysis, adrafinil solutions between 0.5-1000 μM were prepared in H_2O/Acetonitrile 3:7 at pH = 6 (MES, 50 mM). 200 nL of the solutions were added to the zones. Responses from sensor arrays were evaluated by LDA classification for semi-quantitative analysis and Support Vector Machine (SVM) regression for quantitative analysis. Cross-validation results confirms 100% classification (Table S2)

Table S1. The jackknifed classification matrix for qualitative analysis

Jackknifed Classification Matrix

	Acetyl salicyclic acid	Adrafinil	Benzoate	Benzohydroxamic acid	Blank	Deferoxamine	Flurbiprofen	Ibuprofen	Ketoprofen
Acetyl salicyclic acid	7	0	0	0	0	0	0	0	0
Adrafinil	0	7	0	0	0	0	0	0	0
Benzoate	0	0	7	0	0	0	0	0	0
Benzohydroxamic acid	0	0	0	7	0	0	0	0	0
Blank	0	0	0	0	7	0	0	0	0
Deferoxamine	0	0	0	0	0	7	0	0	0
Flurbiprofen	0	0	0	0	0	0	7	0	0
Ibuprofen	0	0	0	0	0	0	0	7	0
Ketoprofen	0	0	0	0	0	0	0	0	7
Mandelic acid	0	0	0	0	0	0	0	0	0
N-hydroxyhexanamide	0	0	0	0	0	0	0	0	0
Total	7	7	7	7	7	7	7	7	7

Jackknifed Classification Matrix (contd...)

	Mandelic acid	N-hydroxyhexana-mide	%correct
Acetyl salicyclic acid	0	0	100
Adrafinil	0	0	100
Benzoate	0	0	100
Benzohydroxamic acid	0	0	100
Blank	0	0	100
Deferoxamine	0	0	100
Flurbiprofen	0	0	100
Ibuprofen	0	0	100
Ketoprofen	0	0	100
Mandelic acid	7	0	100
N-hydroxyhexanamide	0	7	100
Total	7	7	100

Table S2. The jackknifed classification matrix for semi-quantitative analysis.

Jackknifed Classification Matrix

	0.5	1	10	100	1000	200	400	Blank	%correct
0.5	7	0	0	0	0	0	0	0	100
1	0	7	0	0	0	0	0	0	100
10	0	0	7	0	0	0	0	0	100
100	0	0	0	7	0	0	0	0	100
1000	0	0	0	0	7	0	0	0	100
200	0	0	0	0	0	7	0	0	100
400	0	0	0	0	0	0	0	0	100
Blank	0	0	0	0	0	0	0	7	100
Total	7	7	7	7	7	7	7	7	100

7. Microfluidic paper based analytical device study

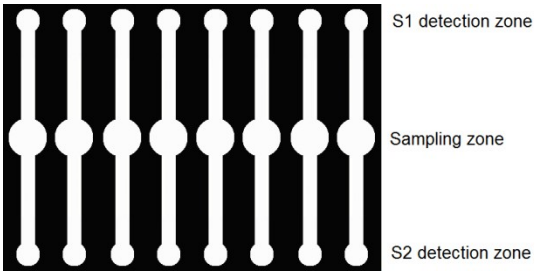

Figure S31. Layout of the microfluidic paper based analytical device (μPAD) with two detection zones (zones at opposite ends) and a sampling zone (middle zone).

The diameter of the detection zones was 2.61 ± 0.04 mm, the diameter of the sampling zone was 4.33 ± 0.05 mm, the length and width of the channels were 10.45x1.65 ± 0.05x0.04 mm, respectively. After printing on chromatography paper (Whatman) with a Xerox ColorQube model 8570 wax printer, the Microfluidic Paper Based Analytical Device (μPAD) was baked for 4.5 min at 110 ^{o}C. The back side of the paper was covered with tape after baking process. On one detection zone 200 nL of Coumarin 343 (500 μM) and 2×200 nL of S1 (10 mM) were injected while 600 nL (3×200nL) of S2 (1 mM) were added on the other detection zone. After evaporation of solvents, 0.75 μL urine sample was applied onto the sampling zone (middle zone). Then 3.25 μL MES buffer (50 mM, pH 6) was applied to sampling zone for eluting adrafinil to the detection zone. Finally, the fluorescence images were recorded on the UV scanner. The fluorescence responses (enhancement in S1 and quenching in S2) were used in construction of calibration curves.

8. Method Validation

The developed method was validated in terms of accuracy, precision, limit of detection (LOD), limit of quantitation (LOQ), range and robustness parameters. LODs and LOQs were calculated by the equations below:

$LOD = 3\sigma / S$

$LOQ = 10\sigma / S$

where σ = standard deviation of the blank responses S = slope of the calibration curve. LOD, LOQ and range values are reported in Table 2 in the main article.

Accuracy was measured by the application of the method to a sample of adrafinil of a known purity, and recoveries are reported in Table S3. Precision was investigated in terms of repeatability and intermediate precision. For repeatability two concentrations of adrafinil were analyzed for 9 times and the relative standard deviations were reported (Table S3). Intra-day precision of these samples are reported. Moreover, different samples were prepared and analyzed by different analysts on different days and by using a different image recorder (Kodak Image Station 440CF and Kodak Image Station 4000MM PRO). F- and t-tests show that there is no significant difference between results of the analysis (Table S3).

Robustness was studied in variations of paper size, pH, concentration of buffer and volume (Table S4). Levels for robustness tests were determined by multiplying the total relative uncertainties for each factor by '5'. The results were evaluated with ANOVA tests and no significant difference was observed between results at p=95% (Table S4).

Table S3. Accuracy and Precision (repeatability and intermediate precision) for urine adrafinil tests

	Intra day				Interday			
	Sensor 1 (n=9)		Sensor 2 (n=9)		Sensor 1 (n=27)		Sensor 2 (n=27)	
	Recovery %	RSD[a]	Recovery %	RSD[a]	Recovery %	RSD[a]	Recovery %	RSD[a]
10 µM	105.6	6.8	104.7	6.6	102.4	6.8	102.0	7.9
500 µM	93.5	3.8	95.0	3.8	99.1	6.2	93.2	9.7

	Experiments 1[b] (n=18) Recovery ± SEM[c]	Experiments 2[b] (n=18) Recovery ± SEM[c]	t test	F test
10 µM	10.21 ± 0.17	10.02 ± 0.15	0.766 (<2.110[d])	1.317 (<2.270[e])
500 µM	484.13 ± 6.86	480.95 ± 9.52	0.281 (<2.110[d])	0.519 (<2.270[e])

[a] RSD: Relative standard deviation %

[b] Intermediate precision experiments were conducted by different analysts, with different samples, in different days and with different instruments

[c] SEM: Standard error of mean

[d] critical t value for α=0.05

[e] critical F calue for α=0.05

Table S4. ANOVA for robustness

Sample Concentration	Paper size[a]			pH			Concentration of buffer (mM)			Sample volume (µL)		
	Big	Normal	Small	5.98	6.00	6.02	49.45	50.00	50.55	0.73	0.75	0.77
	Recoveries (µM)			Recoveries (µM)			Recoveries (µM)			Recoveries (µM)		
10 µM	10.14	10.22	10.26	10.29	10.22	10.06	9.89	10.22	10.25	10.21	10.22	10.24
ANOVA tests	F = 0.0952 (<3.204[b])			F=0.916 (<3.204[b])			F=3.040 (<3.204[b])			F=0.916 (<3.204[b])		

[a] paper sizes were tested detection area 2.61 ± 0.19 mm, sampling area 4.33 ± 0.27 mm, channel length 10.45 ± 0.21, channel width 1.65 ± 0.23 mm

[b] $F_{crit.}$ for d.f. 2 – 45 at α=0.05